Catalysis Today 297 (2017) 308–315

Contents lists available at ScienceDirect

Catalysis Today

journal homepage: www.elsevier.com/locate/cattod

Effect of chlorine on performance of Pd catalysts prepared via colloidal immobilization

Yingnan Zhao[a,c], Wanwei Liang[a], Yongdan Li[b], Leon Lefferts[a,*]

[a] *Catalytic Processes and Materials, Faculty of Science and Technology, MESA+ Institute for Nanotechnology, University of Twente, Enschede, 7500AE, The Netherlands*
[b] *School of Chemical Engineering, Tianjin University, Tianjin, 300072, China*
[c] *Department of Biotechnology and Chemical Technology, School of Chemical Technology, Aalto University, P.O. Box 16100, 00076 Aalto, Finland*

ARTICLE INFO

Article history:
Received 8 November 2016
Received in revised form
28 December 2016
Accepted 17 January 2017
Available online 22 January 2017

Keywords:
Pd catalysts
Nitrite hydrogenation
Chlorine
Colloid
Selectivity

ABSTRACT

This contribution shows the effect of residual chlorine on the catalytic performance of a Pd-based catalyst in the hydrogenation of nitrite for cleaning of drinking water. The catalyst was prepared *via* immobilization a colloidal Pd nanoparticles using activated carbon as support. Different amount of hydrochloric acid (HCl) was added to immobilize the Pd colloid on the carbon support, facilitating the removal of the residual stabilizer, polyvinyl alcohol (PVA), from the surface of the Pd nanoparticles (NPs). The catalysts were characterized by TEM, CO-chemisorption, XRF, N_2 physisorption, UV–vis spectroscopy, and XPS. The activity and selectivity of the catalysts were measured for nitrite hydrogenation in semi-batch operation. The results show that PVA can be removed completely at pH below 2. The residual chlorine on the catalysts can be removed by reduction in H_2/N_2 at a mild temperature, *i.e.* 200 °C, regardless the amount of HCl used. Nevertheless, high concentration of HCl during immobilization (pH 1) causes partial Pd re-dissolution according to UV–vis spectroscopy, resulting in formation of highly dispersed Pd clusters that could not be detected with TEM. Reduction of this catalyst with high chlorine content in H_2 at 200 °C is resulting in formation of relatively large Pd particles via sintering. Without pre-reduction at 200 °C, residual chlorine can also be removed almost completely during the hydrogenation reaction at room temperature. The activity of the Pd catalyst is insensitive to the chlorine concentration below 30 μmol L^{-1} in the aqueous reaction mixture. Interestingly, the selectivity to N_2 is improved by adding chlorine to the reaction mixture, independent of the way chlorine is added, i.e. via the catalyst or added directly to the reaction solution.

1. Introduction

Nitrate and nitrite contamination in groundwater has become a rising risk for supplying of drinking water, especially in agricultural areas where synthetic nitrogen fertilizers are extensively used [1–3]. Catalytic hydrogenation of nitrate/nitrite (Eqs. (1)–(3)) using Pd-based catalysts has been developed since the late 1980s, as a highly efficient method operated under mild conditions (typically around 25 °C and ambient pressure) [4,5]. This method prevents formation of any contaminating brines as in ion-exchange procedures, and is able to convert nitrate and nitrite in water lacking any organic contamination, as is required for biological treatment [6,7].

$$2NO_3^- + 2H_2 \xrightarrow{\text{Pd-Cu}} 2NO_2 + 2H_2O \quad (1)$$

$$2NO_2^- + 3H_2 + 2H^+ \xrightarrow{\text{Pd}} N_2 + 4H_2O \quad (2)$$

$$NO_2^- + 3H_2 + 2H^+ \xrightarrow{\text{Pd}} NH_4^+ + 2H_2O \quad (3)$$

Colloidal method has been developed extensively for preparation of metal nanoparticles (NPs) for catalytic application in the last few decades [8,9]. The advantage of the method is well-known: the sizes of the NPs can be well controlled and manipulated, facilitating studies on structure-performance relationships. Advanced methods allow formation of NPs with well-defined shapes, offering interesting opportunities on even more detailed studies on the influence of surface structure on catalysis [10,11].

---

* Corresponding author.
E-mail address: l.lefferts@utwente.nl (L. Lefferts).

http://dx.doi.org/10.1016/j.cattod.2017.01.028

Pd based catalysts for nitrate/nitrite hydrogenation have been studied using colloid preparation methods [11–16], reporting that the rate of nitrite hydrogenation is independent on Pd particle size [14,17,18]. Nevertheless, it is also well reported that residual stabilizers, such as polyvinyl alcohol (PVA) and polyvinylpyrrolidone (PVP), can block part of the active sites by covering the majority of the metal surface [14,19–22]. Stabilizers and capping agents can also manipulate adsorbed reactive species on metal surface, influencing the activity as well as the selectivity of Pd catalysts [14,22–25]. As a result, it is generally preferred to remove the residual stabilizers on metal surface.

Removal of the residual stabilizers is challenging, normally including oxidation and thermal treatment, making it difficult to maintain particle size and crystal structure of the NPs, and still, the removal can be incomplete [26–30]. In our previous work [13], the Pd colloid was immobilized on activated-carbon (AC) in aqueous HCl solution at pH 2. It was observed that PVA could be completely removed from the Pd surface, according to TEM and CO chemisorption results. It was proposed that extensive chemisorption of Cl on the Pd surface, promoted by the presence of O_2 according to reactions in Eqs. (4) and (5), is weakening the interaction between PVA and the NPs [13].

$$2Pd + O_2 \rightarrow 2PdO \qquad \Delta G = -186.82\,\text{kJ} \tag{4}$$

$$PdO + 2Cl^- + 2H^+ \rightarrow PdCl_2 + H_2O\,(l) \qquad \Delta G = -41.38\,\text{kJ} \tag{5}$$

After the PVA removal, the catalysts were reduced mildly in H_2/N_2 atmosphere at 200 °C, in order to reduce $PdCl_2$ to Pd^0, removing chlorine from the Pd surface. On the other hand, chlorine removal is not complete and a small but significant amount of chlorine remains on catalyst support i.e. activated carbon.

This contribution aims at optimization of the HCl concentration during immobilization of Pd-PVA colloid on activated carbon. The effect of residual chlorine influencing the activity and the selectivity in nitrite hydrogenation will also be shown.

2. Experimental

2.1. Chemicals

Sodium tetrachloropalladate(II) ($Na_2PdCl_4 \geq 99.995\%$ (metal basis)), polyvinyl alcohol (PVA, average MW = 13000–23000, 87%–89% hydrolyzed), sodium borohydride ($NaBH_4$, ≥96% (gas-volumetric)), and formic acid (98%–100%) were purchased from Sigma-Aldrich. Sodium nitrite (>99%) was purchased from Merck. Activated carbon (AC, $S_{BET} = 1000\,m^2\,g^{-1}$) was supplied by Norit. AC was sieved in the range of 38–45 μm in diameter before used as catalyst support. All the aqueous solutions were prepared using ultra purified water obtained (Millipore, Synergy).

2.2. Pd colloid preparation

The preparation of palladium nanoparticles via colloidal method has been described previously, which can be summarized as follows [13]. PVA was dissolved in water at 70 °C with stirring for at least 2 h. The solution (2 wt%) was then cooled down to room temperature. Aqueous solution of Na_2PdCl_4 (20 mL, containing 0.086 mmol Pd) and 1.76 mL of freshly prepared PVA solution were added to 240 mL water, obtaining a yellow-brown solution. After 3 min, $NaBH_4$ solution (1.72 mL, 0.172 mmol) was added under vigorous stirring. The brown Pd colloid solution was immediately formed. The final pH was typically 8–8.5.

2.3. Colloid immobilization

Typically, 0.75 g AC or graphite was added to the Pd colloid solution (260 mL, $3.3 \times 10^{-4}\,mol\,L^{-1}$) immediately after preparation. Hydrochloric acid (HCl) was added to adjust pH to either 1, 2 or 3. The slurry was stirred in air with a mechanical 6-blade-stirrer (ϕ 44 mm, 1000 rpm) with the propeller positioned at the centre of liquid for 2 h at room temperature, filtered and thoroughly washed with water. After that, the catalysts were dried in vacuum at 40 °C overnight.

2.4. Catalyst reduction

Catalysts prepared as described above were carefully treated in a tube furnace. In a typical procedure, the temperature was raised to 200 °C at a rate of $5\,°C\,min^{-1}$, then kept for 1 h at 200 °C, in 10 vol% H_2/90 vol% N_2. Then the sample was flushed in N_2 for 30 min at 200 °C, and cooled down at a rate of $20\,°C\,min^{-1}$ to room temperature in the same atmosphere. The catalysts were flushed in N_2 for 24 h before exposure to air. In the following, the sample notation will be used as shown in Table 1.

2.5. Characterization

Pd particle size distribution was determined using TEM (Philips CM300ST-FEG) allowing reliable detection of metal nanoparticles of 1 nm and lager on AC. The AC supported catalysts were firstly ground into sub-micron fragments and dispersed in ethanol. Then the suspension was dropped on a copper grid covered with hollow carbon for TEM image taking. At least five of these fragments were randomly selected for determination of Pd particle sizes, and typically 300 Pd particles were measured. Note that information on the spatial distribution of nanoparticles through the support cannot be obtained as the samples were ground. The metal loading on the supports were analyzed by XRF. The total surface area of samples were calculated based on N_2 physisorption data, using the BET method for p/p_0 values between 0.03 and 0.13 for catalysts prepared with AC following the recommendations of Rouquerol et al. [31], with a typical error margin of 5%.

Re-dissolution of Pd by HCl was measured with UV–vis spectroscopy of the colloidal suspension in a UV-spectrometer (Perkin Elmer Lambda 850, wavelength from 200 to 800 nm, scanning speed 266.75 $nm\,min^{-1}$) at room temperature. The pH of freshly prepared unsupported Pd-PVA colloid suspension was adjusted to 1, 2 and 3 by adding HCl solution, followed by stirring the suspension in air atmosphere for 2 h. Then 500 μL of the treated suspension was introduced in a quartz cell (QS1000) for performing the measurement.

CO chemisorption at room temperature was used to determine the metal surface area that is accessible in gas phase. Typically, the sample was pre-reduced at room temperature in hydrogen and then flushed in He at the same temperature. Then CO was

Table 1
Sample notations and details of corresponding preparation procedure.

Sample	Preparation Procedure
Pd_AC_1_A	Pd-PVA colloid immobilized on AC using HCl to adjust pH to 1
Pd_AC_2_A	Pd-PVA colloid immobilized on AC using HCl to adjust pH to 2
Pd_AC_3_A	Pd-PVA colloid immobilized on AC using HCl to adjust pH to 3
Pd_AC_1_R	Pd_AC_1_A reduced in H_2/N_2 at 200°C
Pd_AC_2_R	Pd_AC_2_A reduced in H_2/N_2 at 200°C
Pd_AC_3_R	Pd_AC_3_A reduced in H_2/N_2 at 200°C

introduced as pulses and the response was recorded using a TCD detector. We assumed that the stoichiometric ratio of number of adsorbed CO molecules and number of accessible Pd surface atoms is 1: 1. The Pd dispersion (*Pd disp.*) was defined as

$$Pd\ disp. = \frac{\text{number of Pd atoms in the surface of NPs}}{\text{number of Pd atoms in total}} \quad (6)$$

The surface composition of the catalysts was analyzed by X-ray photoelectron spectroscopy (XPS, Quantera SXM, Al $K\alpha$ (1486.6 eV)). The powder samples were stored in air without any further pretreatment before analysis. Typically, a few microgram sample was pressed into an indium foil, and four spots ($600 \times 300\ \mu m^2$) on the sample were randomly selected for measurements to average out any inhomogeneity in the catalysts. The accuracy of the resulting peak positions was within 0.2 eV. The spectra were fitted using the software “Multipak v.9.4.0.7”. Typically, the binding energy in all spectra was first calibrated using the carbon 1 s peak at 284.8 eV as an internal reference. The spectra detected at four spots of one sample were averaged in order to improve the signal-to-noise ratio, followed with Shirley background subtraction. The Pd peaks were fitted using an asymmetric model, necessary because of interaction of the photoelectrons with the valence band electrons [32], whereas the S and Cl peaks were fitted using mixed Gaussian-Lorentzian model, as suggested by Handbook of X-ray Photoelectron Spectroscopy [33]. The peaks for each sample (Pd 5d, Cl 2p and S 2p) were fitted with sets of doublets with identical FHWM. Both width and peak position were allowed to optimize. The distance within the doublets was fixed, according to the data suggested in the handbook [33].

2.6. Nitrite hydrogenation

The reaction was performed in a home-build apparatus including a glass tank reactor (ϕ 98 mm with four 5 mm baffles), equipped with a mechanical 6-blade-stirrer (ϕ 44 mm, 1000 rpm) with the propeller positioned at the centre of liquid. Typically, 50 mg catalyst was added to 300 mL H_2O. The mixed suspension was then stirred vigorously, while a $H_2/He/CO_2$ gas mixture was introduced via a dipped pipe ($H_2/He/CO_2$ = 6/3/1 by volume flow rate, total flow rate = 100 mL min^{-1}, total pressure = 1 bar) for at least 1 h. CO_2 was used as a buffer according to reaction shown in Eqs. (7) and (8) to partly compensate for the protons consumed by nitrite hydrogenation.

$$CO_2 + H_2O \rightarrow HCO_3^- + H^+ \quad (7)$$

Table 2
Summary of XRF elemental analysis, TEM and CO chemisorption.

Sample	C_{Cl} (wt%)[a]	d_{TEM} (nm)	*Pd disp.* (%)	
			CO chemisorption[b]	TEM[c]
Pd_AC_1_A	1.1	3.0 ± 1.2	12 ± 3	30
Pd_AC_2_A	0.8	2.8 ± 0.9	12 ± 2	32
Pd_AC_3_A	0.6	3.1 ± 1.2	8 ± 2	29
Pd_AC_1_R	n.d.[d]	4.1 ± 1.1	32 ± 5	22
Pd_AC_2_R	n.d.	3.0 ± 1.0	30 ± 4	30
Pd_AC_3_R	n.d.	3.2 ± 1.2	18 ± 4	28

[a] Chlorine content in the catalysts according to XRF.
[b] CO chemisorption in gas phase. The samples reduced in H_2 flow for 1 h at 21 ± 1 °C.
[c] Estimated assuming clean spherical Pd NPs.
[d] The content is under XRF detective limitation (<0.05 wt%).

$$HCO_3^- + H_2O \rightarrow CO_3^{2-} + H^+ \quad (8)$$

Then 3 mL 4.2 mmol L^{-1} $NaNO_2$ solution was introduced, starting the reaction. Samples of 1 mL were taken with a syringe every 5 min. Catalysts were removed using a syringe filter (PTFE, 0.2 μm) before injecting into ion chromatograph (DIONEX, ICS 1000) to determine the content of nitrite and ammonium.

3. Results

3.1. Elemental analysis and physical properties

XRF results in Table 2 shows that the chlorine concentration decreased with increasing pH (less HCl used) for as-prepared catalysts. Chlorine content was below the XRF detection limit (<0.05 wt%) after reduction in H_2/N_2 at 200 °C. The Pd content of all catalysts was 1.2 ± 0.1 wt%.

TEM results in Table 2 and Fig. 1 and S-1 show Pd particle sizes of about 3 nm on average in all catalysts, except for Pd_AC_1_R with 4 nm averaged particle size, prepared using the highest HCl concentration and reduced at 200 °C.

CO chemisorption was used to determine the accessibility of Pd surface in gas phase. As shown in Table 2, the apparent dispersions were as low as 10% for all as-prepared catalysts. Note that the samples were first reduced in H_2 flow at room temperature before CO was chemisorbed from gas phase. After reduction in H_2/N_2 at 200 °C, the apparent dispersion was significantly increased, agreeing with our previous observations [13]. Nevertheless, the dis-

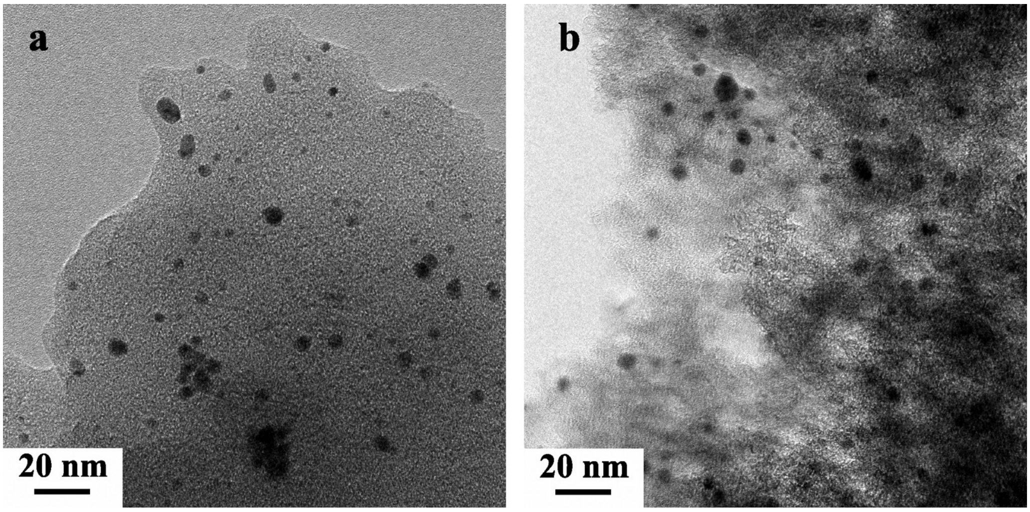

Fig. 1. Typical TEM images of Pd-PVA supported on AC: (a) Pd_AC_1_A; (b) Pd_AC_1_R.

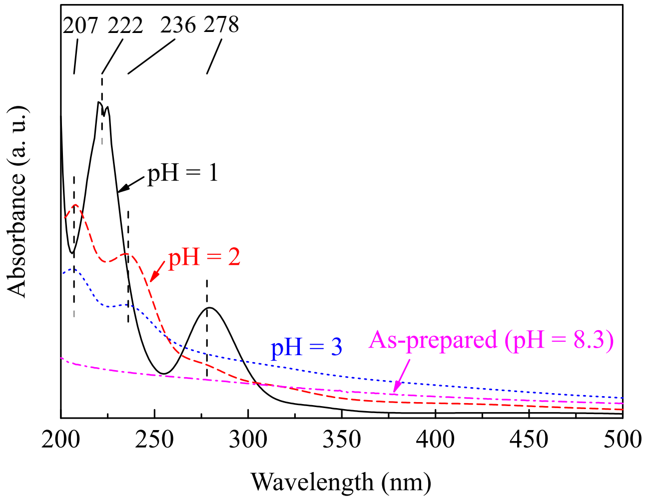

Fig. 2. UV–vis spectra of unsupported Pd-PVA colloid suspension after stirring in air for 2 h at different pH adjusted with HCl. The absorption peaks at 207 nm and 236 nm can be attributed to $[PdCl_3(H_2O)]^-$ and peaks at 222 nm and 278 nm to $[PdCl_4]^{2-}$ [34,35]. Note there is no activated carbon support added in the colloid suspension.

Table 3
XPS results of Pd and Cl oxidation-states and surface concentration.

Sample	Pd^{2+}/Pd	Cl(Pd)/Cl[a]	$Cl(Pd)/Pd^{2+}$
Pd_AC_1_A	0.38	0.75 ± 0.04	1.7
Pd_AC_2_A	0.38	0.79 ± 0.05	1.8
Pd_AC_3_A	0.07	0.72 ± 0.04	3.0
Pd_AC_1_R	0.12	0.37 ± 0.11	2.1
Pd_AC_2_R	0.03	0.43 ± 0.12	3.1
Pd_AC_3_R	0.03	0.36 ± 0.11	1.7

[a] Cl(Pd) stands for chlorine bonded on Pd surface.

persion of the catalyst prepared with pH 3 was only 18% after the reduction, much lower as compared with catalysts prepared with pH 1 and 2 (about 30%).

Figure S-2 shows that PVA is blocking micro-pores exclusively in all catalysts, without influencing meso-pores where the Pd NPs are most probably located, agreeing with the previous study [13].

3.2. UV–vis spectroscopy

Fig. 2 shows partial re-dissolution of Pd for unsupported Pd-PVA colloid stirred in air at different pH controlled by HCl concentration. No Pd-Cl complex was detected in as-prepared colloid suspension, indicating no Pd-containing ions exist right after colloid preparation. After stirring in air for 2 h, $[PdCl_3(H_2O)]^-$ (207 nm and 236 nm) was the only detected Pd-Cl complex in the colloid suspension at low HCl concentration (pH 3). In contrast, $[PdCl_4]^{2-}$ (278 nm) is detected in the suspension at pH 2, becoming the majority Pd-Cl complex (222 nm and 278 nm) when the pH was further decreased to 1 by adding more HCl.

3.3. XPS

XPS results are summarized in Table 3, and typical spectra are shown in Fig. 3 and Figure S-3 in Supporting Information. The results agree with previous observations in general: the surface of Pd NPs was oxidized by formation of $PdCl_2$; reduction in H_2/N_2 at 200 °C reduces Pd^{2+} to Pd^0, while removing chlorine [13]. In addition, the results show that these effect depend on the HCl concentration: while only 7% Pd is oxidized in the as-prepared catalyst prepared with low HCl concentration (pH 3), much higher values are observed (up to 38%) for catalysts prepared with lower pH. It is also shown that as high as 12% Pd is oxidized in catalyst prepared with pH 1 after reduction in H_2/N_2 at 200 °C.

On the other hand, two types of chlorine were detected with formal charge Cl^-, as shown in Fig. 3 and Table 3, which can be attributed to Cl bonded to Pd (*ca.* 198 eV) and Cl in organic compounds presumably present on AC (*ca.* 200 eV), respectively [36]. The amounts of both types of chlorine decreased significantly after reduction at 200 °C in H_2/N_2, whereas the signal of chlorine in organic compounds decreased to lesser extent as compared to chlorine on Pd. Furthermore, the molar ratio of $Cl(Pd)/Pd^{2+}$ was in the range of 2–3 for all samples, both before and after reduction.

3.4. Nitrite hydrogenation

Fig. 4(a) and (b) present concentrations of nitrite and ammonium as function of time. The initial rate per total Pd can be estimated using the Pd loading as determined by XRF in Table 1, as shown in Fig. 4(c). Alternatively, Fig. 4(d) shows the initial rate per surface Pd, where the amount of surface Pd was determined by XRF results together with CO chemisorption results in Table 2. In both cases, the reaction rate showed no significant change with variation of the pH during colloid immobilization for as-prepared Pd-PVA/AC catalysts in Fig. 4(d). For the reduced catalysts, an increase of reaction rate was observed with increasing the pH-value. Additionally, ammonium formation continued after nitrite was converted completely. This was explained in previous work by the presence of residual N-containing species on Pd surface, probably nitrogen atoms, reacting very slowly with hydrogen at close-to-complete conversion level [15]. Consequently, the selectivity of the catalysts to ammonium can only be compared at conversion levels below 100%.

Fig. 5 shows that selectivity to ammonium decreased with increasing pH during colloid immobilization, for both as-prepared and reduced catalysts. The reduction treatment at 200 °C in H_2/N_2 resulted in higher selectivity to ammonium, regardless the amount of HCl used for immobilization.

The amount of Cl introduced by adding the catalysts to the batch reactor ($M_{Cl,cata}$) can be calculated using the XRF results in Table 2, as shown in Table 4. Cl^- is released from the catalyst to the solution during the 1 h pre-reduction treatment, before the reaction is initiated by injection of the nitrite solution. The amounts of Cl^- in aqueous phase detected by IC ($M_{Cl,solu}$) are also shown in Table 4. In all cases, the values of $M_{Cl,cata}$ and $M_{Cl,solu}$ are in good agreement, indicating that chlorine on the catalyst indeed dissolves completely. In order to reveal the influence of the free Cl^- in the reaction solution on catalyst performance, NaCl was added to the reaction slurry with Pd_AC_3_R, as shown in Table 4. The catalyst activity remained constant within experimental error as a result of adding NaCl; surprisingly, the selectivity to ammonium decreased significantly.

4. Discussion

4.1. Influence of HCl on the accessibility of Pd surface

CO chemisorption results in Table 2 show significant increase of accessible Pd surface after reduction in H_2/N_2 at 200 °C for the catalyst prepared at pH 1 and 2, resulting in Pd dispersions similar to the observations with TEM. This confirms that PVA can be removed completely using HCl at pH 2 in the presence of air, as reported previously [13]. After PVA removal via washing and subsequent drying, H_2 reduction at 200 °C removed chlorine from the Pd surface via formation of gaseous HCl, as confirmed by XRF results in Table 2.

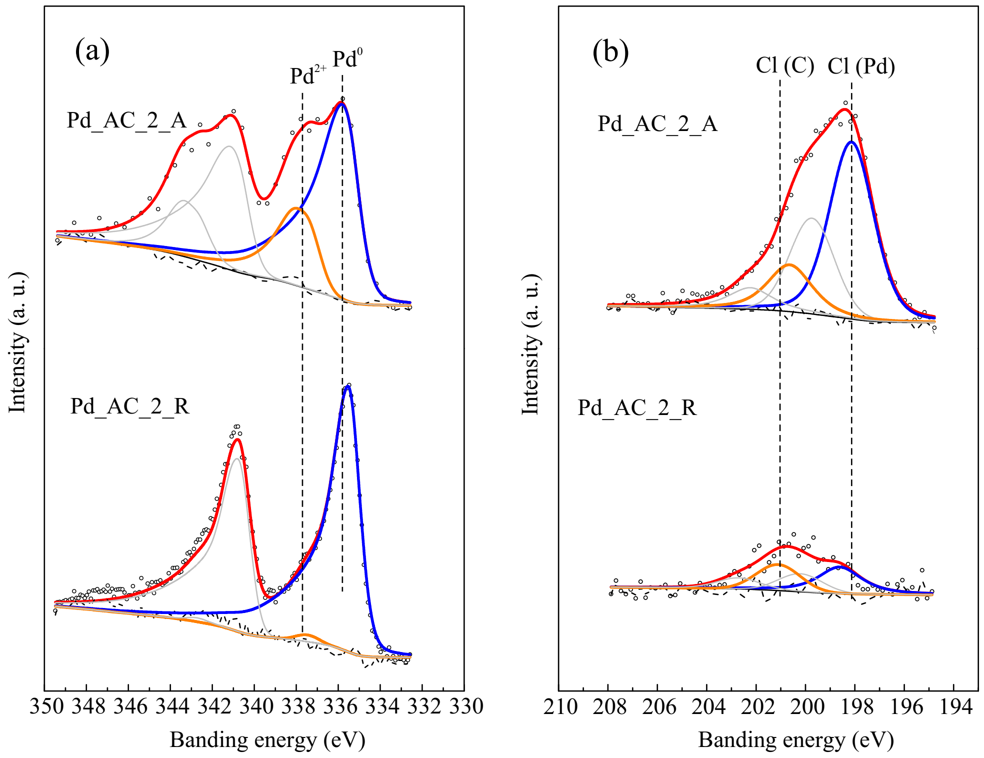

Fig. 3. XPS spectra of activated carbon supported Pd-PVA colloids prepared at pH 2: (a) Pd 3d spectra, (b) Cl 2p spectra. Original data (hollow dots) was subtracted with Shirley background (black line) and fitted using method described in Section 2.5. The fitted Pd 3d5/2 peaks, and Cl 2p3/2 peaks are highlighted (blue and orange) for comparison. The fitted Pd 3d3/2 peaks and Cl 2p1/2 peaks are kept in gray. The sum of all fitted peaks showed as red line with error showed as dash line. Cl(C) and Cl(Pd) stand for chlorine in organic compounds and chlorine bonded on Pd surface, respectively. (For interpretation of the references to colour in this figure legend, the reader is referred to the web version of this article.)

Table 4
Summary of reaction rate and selectivity to ammonium related to chlorine concentration.

Sample	$M_{Cl,cata}$ (μmol)[a]	$M_{Cl,solu}$ (μmol)[b]	Initial rate per total Pd ($mol_{nitrite}\ mol_{Pd}^{-1}\ L^{-1}\ min^{-1}$)	Initial rate per surface Pd ($mol_{nitrite}\ mol_{Pd}^{-1}\ L^{-1}\ min^{-1}$)	NH_4^+ selectivity at 80% conversion (%)
Pd_AC_1_A	16	16	7.7 ± 1.5	62.6 ± 12.5	9.1 ± 0.5
Pd_AC_2_A	11	11	6.0 ± 1.5	51.3 ± 12.8	3.6 ± 0.4
Pd_AC_3_A	8.4	8.0	4.2 ± 1.5	50.7 ± 17.8	0.8 ± 0.2
Pd_AC_3_R	–	0.3	12.6 ± 1.5	71.9 ± 8.5	2.3 ± 0.3
Pd_AC_3_R with extra NaCl		9.2	13.3 ± 1.5	76.1 ± 8.5	1.1 ± 0.2

[a] Amount of Cl introduced by adding the catalyst in the reactor, according to XRF results in Table 2.

[b] Amount of Cl in aqueous phase during reaction detected by IC.

On the other hand, CO chemisorption data in Table 2 also show a relatively low Pd dispersion of 18% on the reduced catalyst prepared with low HCl concentration (pH 3). This apparent dispersion is lower than what would be expected based on TEM and we suggest that this is caused by the presence of PVA. XRF results in Table 2 show a relatively low chlorine concentration in the as-prepared catalyst, in agreement with XPS results in Table 3. In this as-prepared catalysts only 7% of the Pd is oxidized as can be seen in Figure S-3(a); furthermore, the Pd^{2+}: Cl(Pd) molar ratio is 1: 2, indicating that the chlorine coverage is well below one monolayer (about 30%), much lower as compared to catalyst prepared using higher HCl concentration (pH 1 and 2). Obviously, both the low chlorine and Pd^{2+}content are caused by the low HCl concentration used during the preparation. We suggest that the small amount of Cl^- is not sufficient to induce desorption of PVA to the same extent at high Cl^- concentration.

Interestingly, the data in Table 4 reveals that almost all chlorine present on the catalyst desorbed and dissolved during the reaction, based on the similarity between the amount of Cl^- introduced, according XRF, and Cl^- content in aqueous phase in the batch reactor as detected by IC. Apparently, the majority of chlorine can be removed from the catalyst surface during reduction in H_2 in aqueous phase, before nitrite was introduced, by reducing the $PdCl_x$ species to Pd metal and producing HCl. However, this does not rule out small amount of chlorine on Pd can still influence the catalytic reactions, as discussed below in Section 4.3 and 4.4. Additionally, the produced HCl is in such a low concentration (lower than 54 μmol L^{-1} as calculated based on data in Table 4), and cannot influence the pH in the reactor significantly, especially in the presence of CO_2.

In short, a critical amount of chlorine is necessary for PVA removal from the Pd surface. The chlorine concentration in the catalyst is determined by the HCl concentration in the aqueous phase during immobilization of Pd-colloid on the carbon support.

4.2. Influence of HCl on Pd oxidation state and particle size

UV-vis spectra in Fig. 2 show the presence of Cl-containing Pd complex anions in the unsupported colloid suspension after stirring in air with different HCl concentration, and the complexes

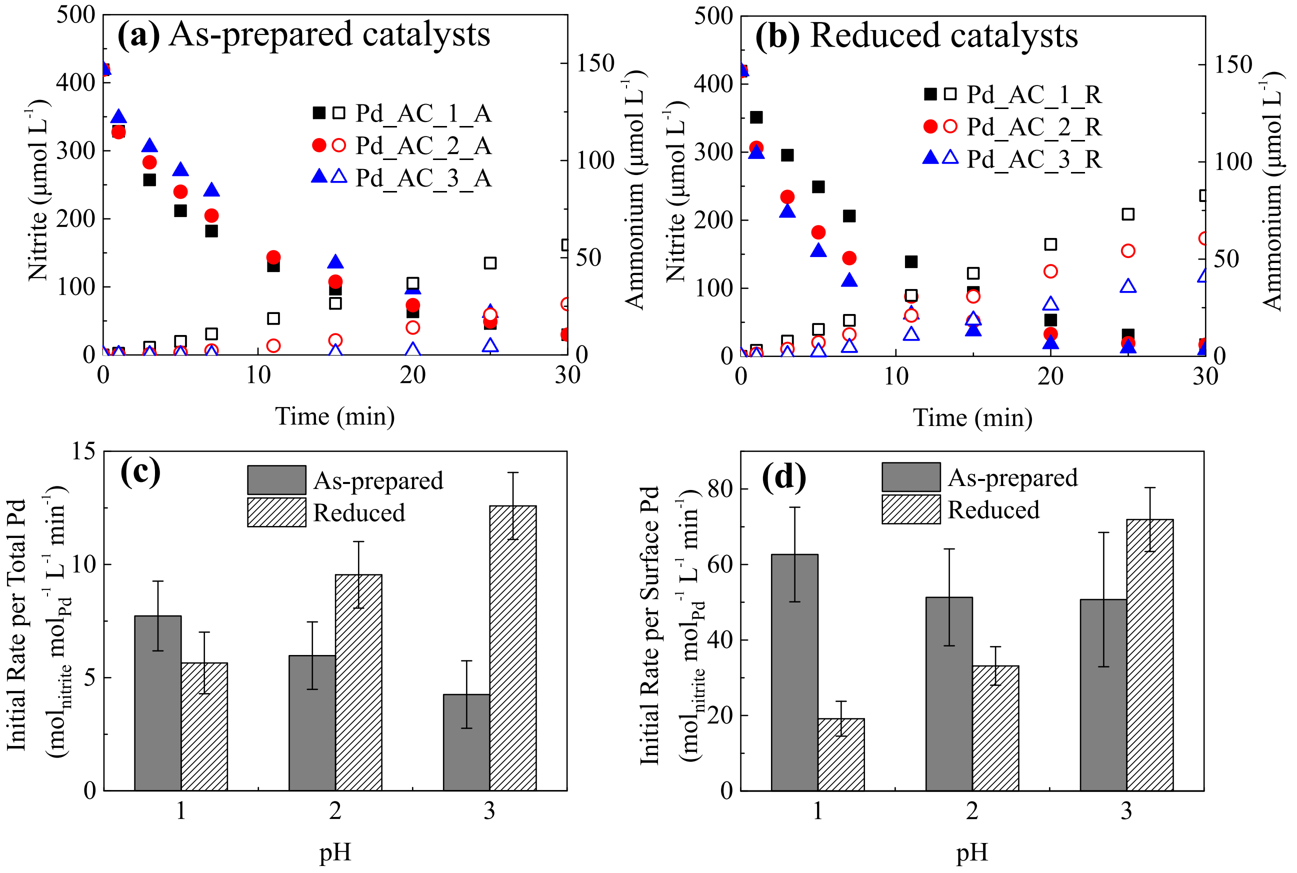

Fig. 4. Activity of Pd-PVA supported on AC before and after reduction at 200 °C in H_2/N_2: concentration of nitrite (solid symbols) and ammonium (open symbols) with (a) as prepared and (b) reduced catalysts; initial reaction rate (c) per total Pd or (d) per surface Pd (in unit of $mol_{nitrite}\ mol_{Pd}^{-1}\ L^{-1}\ min^{-1}$) with catalysts prepared at different pH. The error bars represent standard deviation.

converted from $[PdCl_3(H_2O)]^-$ to $[PdCl_4]^{2-}$ with increasing HCl concentration (i.e., decreasing pH). Apparently, these Pd complex anions originate from partially re-dissolution of the Pd NPs, according to Eq. (9).

$$Pd \xrightarrow[O_2H^+]{+Cl^-} PdCl_2 \xrightarrow[+H_2O]{+Cl^-} [PdCl_3(H_2O)]^- \xrightarrow[-H_2O]{+Cl^-} [PdCl_4]^{2-} \qquad (9)$$

XRF results in Table 2 clearly show very similar Pd loadings for all the catalyst supported on AC, independent of the HCl concentration. This indicates that the majority of dissolved $PdCl_x{\cdot}(H_2O)_{4-x}$ anions ($2 < x \leq 4$) re-adsorb on AC. In this study, the Pd dispersion determined by CO chemisorption, after reduction at 200 °C for 2 h in order to remove chlorine from the Pd nanoparticles, is 32% for the catalyst prepared with the highest HCl concentration (pH 1), significantly higher than the dispersion estimated based on TEM (22%). This indicates the existence of extremely small Pd NPs, which cannot be detected with the TEM used in this study. Simonov et al. reported that $[PdCl_4]^-$ can either form π-complexes of $PdCl_2$ with C=C fragments of the carbon matrix, or be reduced to metallic Pd particles by spontaneous reduction on carbon in the presence of HCl [36–38]. Probably, extremely small Pd and $PdCl_2$ particles are formed in the same way here. On the other hand, TEM shows even larger Pd particles with an average size of 4 nm in the sample Pd_AC_1_R, indicating some sintering during reduction in H_2/N_2 at 200 °C.

Surprisingly, as high as 12% of Pd atoms remained oxidized after reduction in H_2/N_2 at 200 °C for 2 h with catalyst prepared with the highest HCl concentration (pH 1), according to XPS results in Table 3 and Figure S-3. As comparison, only 3% of Pd was oxidized in reduced catalysts prepared at pH 2 and 3. All catalysts were kept in ambient overnight before XPS performed. The high amount of oxidized Pd in the reduced catalyst prepared with pH 1 is supporting the suggestion that very small Pd particles are present, as these are more susceptible for oxidation in ambient.

In summary, excess amount of HCl causes partial re-dissolution of Pd NPs, causing increasing Pd particle sizes as well as residual $PdCl_2$ after reduction by H_2. Thus a moderate amount of HCl should be used to remove PVA from Pd surface completely, at the same time minimizing side-effects caused by extra HCl.

4.3. Influence of HCl on activity

4.3.1. Influence of chlorine on the activity of as-prepared catalysts

As shown in Fig. 4(c) and (d), all as-prepared catalysts showed similar activity within experimental error, regardless the different chlorine concentrations. Accordingly, XRF results in Table 2 and IC results in Table 4 show the majority of chlorine re-dissolved in aqueous phase during the reduction treatment in the reactor, immediately before the catalytic experiment, cleaning the Pd surface and making the surface Pd atoms accessible for reactants. Furthermore, no significant change in activity for Pd_AC_3_R was found when adding chlorine up to 9.2 µmol (30 µmol L^{-1}) as shown in Table 4. Apparently, chlorine dissolved in the reaction mixture at the concentrations in this study has no significant influence on the apparent activity.

At first sight this seems to disagree with results reported by Pintar, et al. on nitrate hydrogenation on Pd/Al_2O_3 [39] and Chaplin et al. on nitrite hydrogenation [40]. In both studies reaction rates decrease with chlorine addition; it should be noted though that the chlorine concentration in this study is at least two order of

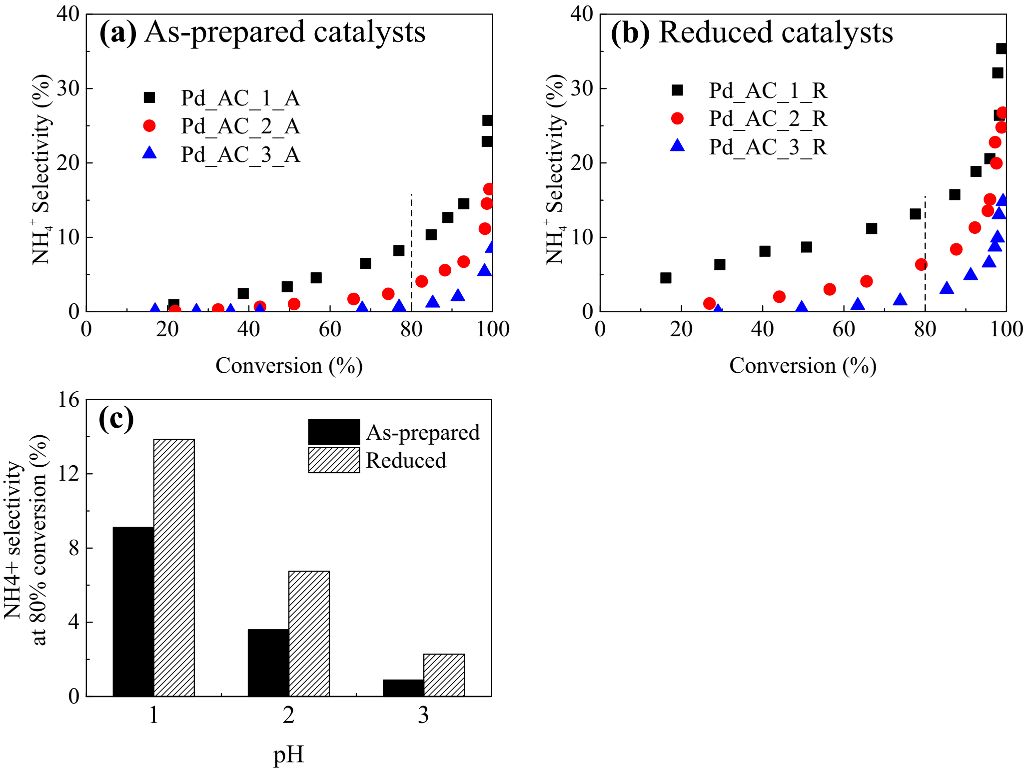

Fig. 5. Selectivity to ammonium for nitrite hydrogenation with Pd-PVA supported on AC: (a) selectivity to ammonium as function of nitrite conversion with as-prepared catalysts; (b) selectivity to ammonium as function of nitrite conversion with catalysts reduced at 200 °C in H_2/N_2; (c) comparison of ammonium selectivity at 80% nitrite conversion with catalyst prepared at different pH.

magnitude lower, explaining why the effect on catalyst activity is negligible.

4.3.2. Activity after reduction

The activity of the catalysts after reduction in H_2/N_2 at 200 °C is compared in Fig. 4(c) and (d). The initial rates of the reaction increase with increasing pH, using less HCl during immobilization of the colloid. It is clear from the discussion above that dissolution and re-deposition of Pd is likely to occur during immobilization of the colloid, probably influencing the particle size distribution of Pd NPs on the support, especially in the case of high HCl concentration (low pH). Possibly, extremely small Pd particles induce a lower activity per active site, as particle size effect have been experimentally excluded exclusively for metal particles larger than 2.5 nm [14,17,18]. This hypothesis needs to be further tested using catalyst with narrow particle size distribution below 2 nm to even atomic level.

In summary, catalyst prepared with lowest HCl concentration (pH 3) results in the highest activity after reduction in H_2/N_2, despite incomplete removal of PVA from the Pd surface. Instead, the re-dissolution of Pd in presence of high HCl concentration in air may cause the decrease of the activity despite complete removal of the polymer.

4.4. Effect of HCl on the selectivity to ammonium

Reduction in H_2/N_2 at 200 °C increases the selectivity to ammonium as shown in Fig. 5(c), together with removal of chlorine content as detected by XRF in Table 2 and XPS in Table 3. On the other hand, Table 4 shows the selectivity decreases with adding extra NaCl in Pd_AC_3_R catalyst. Clearly, Cl^- decreases the selectivity to ammonium, no matter whether Cl^- is released from the catalyst during the reaction or is added to the aqueous phase reaction mixture. A reliable comparison to similar effects reported in literature is not possible, again because the concentration of chlorine in this study is much lower than in literature [39,40].

Surprisingly, the selectivity to ammonium increased with increasing HCl concentration during colloid immobilization, for both as-prepared and reduced catalysts, as shown in Fig. 5. Table 4 confirms that catalysts prepared with higher HCl concentration induced higher chlorine concentration during the catalytic reaction. Clearly, this disagrees with the effect of the Cl^- concentration in the reaction mixture as discussed above and therefore another effect on selectivity apparently contributes.

It was found in our previous work [14] that PVA is not influencing the selectivity whereas the selectivity to ammonium increases with increasing Pd particle size. Therefore, we suggest that the selectivity is influenced via the metal particle size as the particle size distributions might be different, as discussed above, influenced by the dissolution and re-deposition of Pd in presence of HCl. Clearly, more work would be needed to test this hypothesis.

In short, the selectivity to ammonium decreases with adding low concentration of chlorine in the reaction mixture, whereas the selectivity to ammonium increases with increasing concentration of HCl during colloid immobilization.

5. Conclusion

Pd-PVA colloids have been immobilized on AC with different HCl concentration in the presence of air. High concentration of HCl (pH 1) used during colloid immobilization causes partial dissolution of Pd, decreasing activity for nitrite hydrogenation and increasing selectivity to ammonium. In contrast, high activity and low selectivity to ammonium can be achieved by using low concentration of HCl (pH 3) during colloid immobilization, despite the fact that PVA can only be partly removed from the Pd particles. Finally, low concentration of free Cl^- in the reaction mixture induces a decreasing selectivity to ammonium, without influencing the reaction rate.

Appendix A. Supplementary data

Supplementary data associated with this article can be found, in the online version, at http://dx.doi.org/10.1016/j.cattod.2017.01.028.

References

[1] European Environment Agency (EEA), http://www.eea.europa.eu/data-and-maps/figures/nitrate-concentration-in-groundwater (Last updated 01 Jan 2002).

[2] B. Gu, Y. Ge, S.X. Chang, W. Luo, J. Chang, Glob. Environ. Change 23 (2013) 1112–1121.

[3] A. Scheidleder, J. Grath, G. Winkler, U. Stärk, C. Koreimann, C. Gmeiner, S. Nixon, J. Casillas, P. Gravesen, J. Leonard, M. Elvira, Eur. Environ. Agency (EEA) (1999).

[4] K.-D. Vorlop, T. Tacke, Chem. Ing. Tech. 61 (1989) 836–837.

[5] T. Tacke, Dissertation, Technischen Universität Carolo-Wilhelmina, 1991.

[6] A. Kapoor, T. Viraraghavan, J. Environ. Eng. 123 (1997) 371–380.

[7] N. Barrabés, J. Sá, Appl. Catal. B 104 (2011) 1–5.

[8] Y. Xia, Y. Xiong, B. Lim, S.E. Skrabalak, Angew. Chem. Int. Ed. 48 (2009) 60–103.

[9] G. Somorjai, J. Park, Top. Catal. 49 (2008) 126–135.

[10] B. Roldan Cuenya, Acc. Chem. Res. 46 (2013) 1682–1691.

[11] D. Shuai, D.C. McCalman, J.K. Choe, J.R. Shapley, W.F. Schneider, C.J. Werth, ACS Catal. 3 (2013) 453–463.

[12] K.A. Guy, H. Xu, J.C. Yang, C.J. Werth, J.R. Shapley, J. Phys. Chem. C 113 (2009) 8177–8185.

[13] Y. Zhao, L. Jia, J.A. Medrano, J.R.H. Ross, L. Lefferts, ACS Catal. 3 (2013) 2341–2352.

[14] Y. Zhao, J.A. Baeza, N. Koteswara Rao, L. Calvo, M.A. Gilarranz, Y.D. Li, L. Lefferts, J. Catal. 318 (2014) 162–169.

[15] Y. Zhao, N. Koteswara Rao, L. Lefferts, J. Catal. 337 (2016) 102–110.

[16] J.K. Chinthaginjala, A. Villa, D.S. Su, B.L. Mojet, L. Lefferts, Catal. Today 183 (2012) 119–123.

[17] D. Shuai, J.K. Choe, J.R. Shapley, C.J. Werth, Environ. Sci. Technol. 46 (2012) 2847–2855.

[18] J.K. Chinthaginjala, J.H. Bitter, L. Lefferts, Appl. Catal. A 383 (2010) 24–32.

[19] A. Villa, D. Wang, D.S. Su, L. Prati, Chemcatchem 1 (2009) 510–514.

[20] A. Quintanilla, V.C.L. Butselaar-Orthlieb, C. Kwakernaak, W.G. Sloof, M.T. Kreutzer, F. Kapteijn, J. Catal. 271 (2010) 104–114.

[21] X. Wang, P. Sonström, D. Arndt, J. Stöver, V. Zielasek, H. Borchert, K. Thiel, K. Al-Shamery, M. Bäumer, J. Catal. 278 (2011) 143–152.

[22] J.N. Kuhn, C.-K. Tsung, W. Huang, G.A. Somorjai, J. Catal. 265 (2009) 209–215.

[23] B. Feng, Z. Hou, H. Yang, X. Wang, Y. Hu, H. Li, Y. Qiao, X. Zhao, Q. Huang, Langmuir 26 (2010) 2505–2513.

[24] Z. Niu, Y. Li, Chem. Mater. 26 (2014) 72–83.

[25] S. Campisi, D. Ferri, A. Villa, W. Wang, D. Wang, O. Kröcher, L. Prati, J. Phys. Chem. C 120 (2016) 14027–14033.

[26] J.A. Lopez-Sanchez, N. Dimitratos, C. Hammond, G.L. Brett, L. Kesavan, S. White, P. Miedziak, R. Tiruvalam, R.L. Jenkins, A.F. Carley, D. Knight, C.J. Kiely, G.J. Hutchings, Nat. Chem. 3 (2011) 551–556.

[27] M. Crespo-Quesada, J.-M. Andanson, A. Yarulin, B. Lim, Y. Xia, L. Kiwi-Minsker, Langmuir 27 (2011) 7909–7916.

[28] Y. Borodko, H.S. Lee, S.H. Joo, Y. Zhang, G. Somorjai, J. Phys. Chem. C 114 (2009) 1117–1126.

[29] C. Aliaga, J.Y. Park, Y. Yamada, H.S. Lee, C.-K. Tsung, P. Yang, G.A. Somorjai, J. Phys. Chem. C 113 (2009) 6150–6155.

[30] A.M. Venezia, V. La Parola, G. Deganello, B. Pawelec, J.L.G. Fierro, J. Catal. 215 (2003) 317–325.

[31] F. Rouquerol, J. Rouquerol, K. Sing, Adsorption by Powders and Porous Solids, Academic Press London, 1999, pp. 237–285.

[32] David Briggs, J.T. Grant, Surface Analysis by Auger and X-Ray Photoelectron Spectroscopy, IM Publications, Chichester, 2003.

[33] J.F. Moulder, W.F. Stickle, P.E. Sobol, K.D. Bomben, Handbook of X-ray Photoelectron Spectroscopy, Perkin-Elmer Corporation, Eden Prairie, 1992.

[34] L.I. Elding, Inorg. Chim. Acta 6 (1972) 647–651.

[35] C. Drew Tait, D.R. Janecky, P.S.Z. Rogers, Geochimica et Cosmochimica Acta 55 (1991) 1253–1264.

[36] P.A. Simonov, A.V. Romanenko, I.P. Prosvirin, E.M. Moroz, A.I. Boronin, A.L. Chuvilin, V.A. Likholobov, Carbon 35 (1997) 73–82.

[37] P. Simonov, S. Troitskii, V. Likholobov, Kinet. Catal. 41 (2000) 255–269.

[38] H. Chu, J. Wang, L. Ding, D. Yuan, Y. Zhang, J. Liu, Y. Li, J. Am. Chem. Soc. 131 (2009) 14310–14316.

[39] A. Pintar, M. vetinc, J. Levec, J. Catal. 174 (1998) 72–87.

[40] B.P. Chaplin, E. Roundy, K.A. Guy, J.R. Shapley, C.J. Werth, Environ. Sci. Technol. 40 (2006) 3075–3081.